photonics

Article

Next-Generation Dual Transceiver FSO Communication System for High-Speed Trains in Neom Smart City

Yehia Elsawy [1], Ayshah S. Alatawi [2,3,*], Mohamed Abaza [1], Azza Moawad [4] and El-Hadi M. Aggoune [3]

1 Electronics and Communication Engineering Department, Arab Academy for Science, Technology, and Maritime Transport, Giza 12577, Egypt; y.sawy13722@student.aast.edu (Y.E.); mohamed.abaza@aast.edu (M.A.)
2 Department of Physics, Faculty of Science, University of Tabuk, Tabuk 71491, Saudi Arabia
3 Artificial Intelligence and Sensing Technology (AIST) Research Center, University of Tabuk, Tabuk 71491, Saudi Arabia; haggoune.aist@ut.edu.sa
4 Electronics and Communication Engineering Department, Arab Academy for Science, Technology, and Maritime Transport, Cairo 11361, Egypt; azza.kamal@aast.edu
* Correspondence: ase.alatawi@ut.edu.sa

Abstract: Smart cities like Neom require efficient and reliable transportation systems to support their vision of sustainable and interconnected urban environments. High-speed trains (HSTs) play a crucial role in connecting different areas of the city and facilitating seamless mobility. However, to ensure uninterrupted communication along the rail lines, advanced communication systems are essential to expand the coverage range of each base station (BS) while reducing the handover frequency. This paper presents the dual transceiver free space optical (FSO) communication system as a solution to achieve these objectives in the operational environment of HSTs in Neom city. Our channel model incorporates log-normal (LN) and gamma–gamma (GG) distributions to represent channel impairments and atmospheric turbulence in the city. Furthermore, we integrated the siding loop model, providing valuable insights into the system in real-world scenarios. To assess the system's performance, we formulated the received signal-to-noise ratio (SNR) of the network under assumed fading conditions. Additionally, we analyzed the system's bit error rate (BER) analytically and through Monte Carlo simulation. A comparative analysis with reconfigurable intelligent surfaces (RIS) and relay-assisted FSO communications shows the superior coverage area and efficiency of the dual transceiver model. A significant reduction of up to 76% and 99% in the number of required BSs compared to RIS and relay, respectively, is observed. This reduction leads to fewer handovers and lower capital expenditure (CAPEX) costs.

Keywords: Neom smart city; high-speed trains; free space optical communication; siding loop; sustainable mobility

Citation: Elsawy, Y.; Alatawi, A.S.; Abaza, M.; Moawad, A.; Aggoune, E.-H.M. Next-Generation Dual Transceiver FSO Communication System for High-Speed Trains in Neom Smart City. *Photonics* **2024**, *11*, 483. https://doi.org/10.3390/photonics11050483

Received: 6 April 2024
Revised: 8 May 2024
Accepted: 13 May 2024
Published: 20 May 2024

1. Introduction

Smart cities are urban environments that harness the power of technology and data to create sustainable, efficient, and livable communities. These cities integrate cutting-edge digital infrastructure, advanced technologies, and intelligent systems to optimize various aspects of urban life. Through the use of sensors, connected devices, and data analytics, smart cities collect real-time information about transportation, energy usage, waste management, public safety, and more. This wealth of data enables city planners and administrators to make informed decisions and implement targeted strategies to improve the quality of life for residents. Furthermore, smart cities are not just limited to technological advancements but also emphasize social innovation and sustainability. They strive to create equitable communities by focusing on affordable housing, accessible healthcare, education, and social services for all residents. By fostering collaboration between government, businesses, academia, and citizens, smart cities foster innovation and entrepreneurship, attracting investments and creating job opportunities in emerging industries [1].

The effective and eco-friendly advancement of cities and their surrounding urban areas has emerged as a critical and widely discussed matter, with a key focus on establishing a transportation system that ensures intelligent and sustainable mobility. According to the United Nations, an astounding three million individuals relocate from rural regions to cities around the globe each week, resulting in an anticipated doubling of urban populations by the year 2050. This rapid urban growth raises significant concerns regarding the capacity of urban areas to accommodate this influx in the forthcoming decades, encompassing the challenges of housing, energy, traffic infrastructure, and deteriorating air quality. The pursuit of sustainable and intelligent solutions for urban transportation aligns with the United Nations' Sustainable Development Goals (SDGs). With the endorsement of the 2030 Agenda, the United Nations has outlined 17 SDGs aimed at addressing global sustainability challenges related to poverty, inequality, and environmental degradation. In 2015, these SDGs were embraced by all 193 member countries of the United Nations, recognizing that attaining these ambitious sustainability objectives necessitates both financial and non-financial commitments from policymakers, entrepreneurs, consumers, and society at large [2].

Urban mobility in smart cities is pivotal for sustainable and efficient urban development. By leveraging advanced technologies and data-driven solutions, smart cities aim to optimize transportation systems, enhance connectivity, and improve residents' quality of life. From intelligent traffic management to shared mobility services, these cities deploy diverse tools to streamline mobility and reduce carbon emissions. Integration of emerging technologies like autonomous vehicles and electric mobility promises to transform urban transportation further. Through innovative policies and partnerships, smart cities strive to create vibrant, accessible, and environmentally sustainable urban environments [3].

High-speed railways (HSRs) play a crucial role in the development of smart cities, offering rapid and efficient transportation solutions for urban residents and visitors alike. With their ability to connect distant urban centers seamlessly, HSRs facilitate mobility and promote economic growth within smart city networks. These advanced transportation systems leverage cutting-edge technology to ensure safety, reliability, and sustainability. By reducing travel times and congestion, HSRs contribute to improved urban mobility and enhance overall accessibility within smart cities. Furthermore, their integration with other modes of transportation, such as metro systems and autonomous vehicles, creates a comprehensive and interconnected urban mobility ecosystem [4].

Neom's ambitious plans encompass the implementation of a high-speed railway system, known as the SPINE or Connector, within its urban framework. This extensive transportation network will stretch over a length of 170 km and assume the role of the city's primary transportation backbone. Remarkably, this advanced system will facilitate swift travel across the entire cityscape, reducing travel time to mere minutes. Engineered to achieve speeds of up to 300 km per hour, the SPINE will stand as a testament to exceptional engineering prowess. Its emphasis on velocity will obviate the necessity for private vehicles, thereby fostering a sustainable urban environment devoid of car dependency. Beyond its transportation function, the SPINE will epitomize Neom's steadfast dedication to sustainability. By employing clean energy sources, the rail system will prioritize efficiency and endeavor to minimize environmental impact. Neom's visionary aspiration will be to revolutionize urban transportation through the implementation of the SPINE, thereby establishing a novel benchmark for sustainable cities [5]. In summary, our manuscript provides the following core contributions:

- Developing the dual transceiver FSO communication system considering both LN and GG channel models, aiming to precisely depict path loss attenuation, pointing misalignment, and the varying intensities of turbulence (weak, moderate, and strong) within the specific conditions of the Neom smart city.

- Extending the scope of our research involves the inclusion of the siding loop scenario in the single-line track (a siding loop refers to a section of a railway track that branches off from the main line and forms a loop or parallel track; it is designed to allow trains traveling in opposite directions to pass each other without disrupting the main flow of traffic), introducing a unique element that enhances the system's practicality and yields valuable insights into its real-world performance. Notably, to the best of our knowledge, this specific aspect has not been considered in any other existing systems.
- Analyzing and computing the received SNR in relation to coverage distance, along with the BER for both channels, offers valuable insights into the system's performance. This is achieved through the use of analytical expressions and validated results obtained via Monte Carlo simulations.
- Carrying out a comparative analysis with both RIS-assisted FSO and relay-assisted FSO systems, showcasing that our proposed model demonstrates superior performance in coverage area and required infrastructure.

The subsequent sections of the paper are structured in the following manner: Section 2 presents a comprehensive review of the relevant literatures and research. Section 3 of the paper introduces the description of the dual transceiver model, as well as the siding loop scenario and the handover procedure. Section 4 presents channel modeling using LN and GG models, considering the atmospheric turbulence of the Neom smart city. In Section 5 performance analysis is conducted for different channel models. Numerical results are explained in Section 6. Furthermore, a comparative analysis is conducted, comparing the results with the aforementioned existing FSO systems, and emphasizing the achieved improvements. In conclusion, Section 7 provides a concise summary of the key findings and contributions of the research.

2. Related Works

Effective telecommunication plays a vital role in the performance of railway transportation within smart cities, given the extensive scale, large distances, numerous employees and passengers, and their continuous mobility. The importance of communication technologies in the railway system is evident in multiple aspects, including the provision of accurate and real-time train location information and facilitating the simultaneous operation of multiple trains on the same track. This importance underscores the essential role of efficient telecommunication in optimizing the efficiency and effectiveness of railway transport systems within smart cities [6].

Despite the progress made in communication technologies, ensuring optimal quality of service (QoS) for forthcoming HSTs remains a formidable task. The main challenges arise from the dynamic nature of wireless channels, which are characterized by frequent fluctuations over time and non-stationarity. In addition to the aforementioned factors, other challenges that affect QoS include co-channel interference, significant path loss attenuation in millimeter-wave and terahertz frequency bands, frequent handovers due to limited coverage area for each BS, and notable doppler shifts. Consequently, it becomes crucial to address these issues effectively to ensure dependable and efficient communication for HSTs [7,8].

Optical wireless communication emerges as a promising wireless access technology that offers potential solutions to the challenges faced by proposed radio frequency (RF) wireless systems in HSTs. Its aim is to satisfy the expanding need for high-quality multimedia services in HSR systems. These advantages include access to a vast unregulated spectrum, immunity to electromagnetic interference, enhanced security due to the inability of optical beams to penetrate opaque objects, and the ability to achieve high capacity per unit volume through frequency reuse. FSO systems are well-suited for environments where the utilization of RF-based systems is constrained or prohibited, including hospitals, airplanes, and military locations, where RF signals may cause interference with monitoring equipment. The versatility of FSO technology allows for its deployment in both indoor and outdoor settings, facilitating the transmission of extremely high data rates reaching up to gigabits per second [9–17].

Hideki et al. [18] presented a ground-to-train (G2T) FSO communication system designed for high data rates. The system demonstrates rapid acquisition time and high-speed handover, achieving approximately 100 ms. It also attains impressive data rates of around 1 Gb/s. The authors of [18] discuss the utilization of acquisition–tracking–pointing (ATP) mechanism and handover techniques to ensure continuous connectivity. The concept of G2T in FSO communication utilizing a Gaussian laser beam was explored by the authors in [19]. They introduced a mathematical model to address the communication link, considering the challenges associated with train aerodynamics. The presented system offers a promising solution for facilitating high-bandwidth communication between the BSs and trains, thereby enabling internet services for train passengers. In [20], a G2T FSO system is implemented by placing light-emitting diodes (LEDs) at BSs positioned along the tracks to illuminate the approaching trains with optical signals. LEDs are selected as the optical source because of their safe and wide emission properties. The authors of [21] proposed a scheme where a rotating transceiver is used for FSO communication in G2T environments. The objective of this scheme was to overcome the difficulties associated with frequent handovers and alignment problems in HST environments. Accordingly, a mechanical gimbal system is employed to rotate the transceivers located on both the train and BSs. This innovative approach ensures uninterrupted line-of-sight (LOS) communication.

Further, Tao Han and Nirwan Ansari introduced a solution known as radio over fiber as an antenna extender (RADIATE) to deliver high-speed internet services to HSTs through cellular networks. RADIATE employs a fiber-based antenna system installed on the train's roof to extend coverage and facilitate smooth handovers between BSs [22]. Kaymak et al. [23] evaluated how laser divergence angles affect the performance of G2T FSO communications. They suggested the employment of a wide beam to alleviate the complexity of the ATP system in FSO transceivers. This approach helps in mitigating the adverse effects caused by train vibrations by utilizing a recommended range of divergence angles for the wide beam. Fan et al. [24] utilized a dual transceiver scheme that was implemented in the G2T communications system. In this arrangement, each BS was equipped with two transceivers capable of orienting in different directions. The study considered only the presence of additive white gaussian noise (AWGN) in the communication channel. A study is conducted in [25] to analyze the performance of G2T FSO links in the context of tropical climate. The objective was to specifically examine rain attenuation and explore techniques to mitigate its effects. Moreover, they proposed an alternative approach to enhance the FSO link model for G2T communications. Their proposal involved implementing multiple transmitters at each BS [26].

Nithin et al. [27] put forward a coverage model for G2T communications utilizing FSO technology. The model adopts a sectorized multi-beam approach and incorporates a smaller divergence angle to minimize geometric losses. Additionally, the system considers atmospheric attenuation to ensure accurate performance evaluation. In [28], the authors introduced a system that tackles challenges related to precise beam tracking and time synchronization between the transmitter and receiver. They introduced an innovative approach for sequence blind detection, utilizing multiple samplers at the receiver to detect on–off keying (OOK) signals. Nithin et al. [29] explored the use of relayed FSO for G2T communications. Their objective was to address network layer handover challenges by examining the performance of optical amplify and forward and optical–electronical–optical regenerate and forward schemes. Pouya et al. [30] proposed an RIS-assisted FSO communication system for HSTs; the proposed system achieved a higher data rate for both fixed-oriented reflection and dynamic-oriented reflection scenarios of RIS.

3. System Description

The FSO communication system comprises three key stages: an optical signal transmitter, a free-space transmission channel, and a receiver. To facilitate full-duplex communication, two transceivers are equipped on both the BS and the train. A visual representation of the line-of-sight considerations for a dual transceiver optical wireless G2T communication link operating on a single straight-line track is shown in Figure 1. On top of the train, there are two strategically placed optical transceivers, one at the front and one at the back. These transceivers are separated by a distance L_T, which represents the length of the train. Similarly, two transceivers are installed at each BS to ensure coverage in both right and left directions. Between the two coverage areas of the BS, there is a coverage gap area L_2. In order to maintain an unobstructed LoS connection between the BS and the train, the BS transceivers are tilted with angle γ, which represents the tilt angle between the optical beam axis and the parallel horizontal track axis [24].

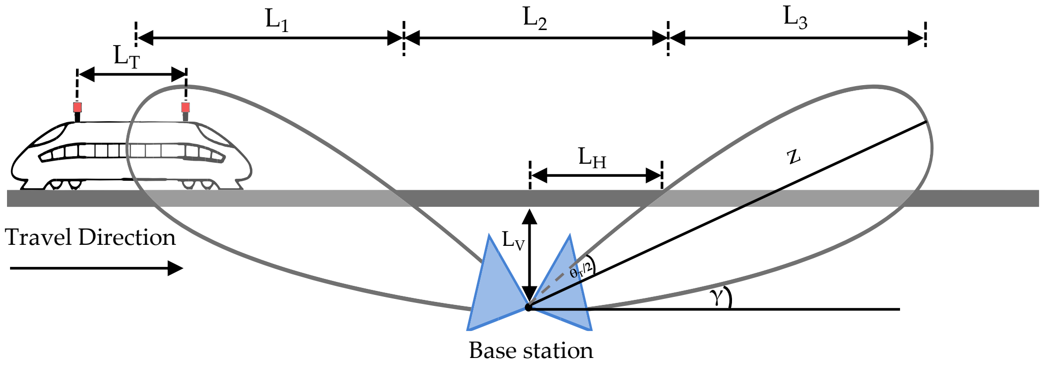

Figure 1. Dual transceiver G2T communication link model.

The BSs are placed at distance L_v away from the track. The BSs are linked to the fiber cable of the network backbone, enabling smooth distribution of data to the Centralized Traffic Controller (CTC). The CTC plays a crucial role in managing the system to enhance network performance and ensure efficient operations [31]. The BSs operate in an on–off mode, activating only when the train is within their transmission range in order to conserve energy. The laser beams emitted with divergence angle θ_T from the BSs are precisely focused on the roof of the train, propagating over a transmission distance z defined as [19]:

$$z = L_c \cos(\gamma) + \sqrt{L_v^2 + L_H^2}\,\cos(\theta_T/2) \tag{1}$$

where L_c represents the track's effective coverage distance for single transceiver and L_H represents the horizontal distance between the BS and the minimum coverage point of the laser source.

3.1. Handover Process

During the train's journey along the track according to Figure 1, a line-of-sight connection between the HST and the BS is consistently maintained. This is achieved by utilizing the geometrical properties illustrated in Figure 1. To ensure uninterrupted connectivity between the BS and the train, the two transceivers placed on the train work together. As the train moves through the coverage distance of a BS, the cooperative behavior of these transceivers guarantees that at least one of them remains connected to the BS. Although the two laser beams of the BSs do not cover the entire railway seamlessly, continuous G2T FSO communication remains unaffected. Here is how it works:

- Once the transceiver at the front of the train is within range of the BS, it forms a connection link with the BS.
- When entering the coverage gap are L_2, the CTC promptly transfers all network traffic to the back transceiver, which is already within. Despite the front transceiver passing through the coverage gap area for a specific period of time, the BS maintains service to the train using the FSO link of the back transceiver.

- Once the front transceiver reaches, which is within the range of other transceiver of the BS, it establishes a connection link with the BS. Subsequently, the CTC allocates the network traffic back to the front transceiver. In order to maintain uninterrupted communication between the BS and the train, the back transceiver must also reach before the front transceiver leaves that particular area.

By employing this approach between the train's front and back transceiver, continuous communication between the BS and the train is maintained throughout the journey. Then the total coverage distance for the dual transceiver BS can be expressed as:

$$L_{C_{total}} = L_1 + L_2 + L_3 = 2L_c + 2L_H \tag{2}$$

3.2. Siding Loop Scenario

As part of our design strategy to enhance the practicality of the system, we considered incorporating siding loops with length L_s in Figure 2, where the BS equipped with two transceivers located at the midpoint of the siding loop $\frac{L_s}{2}$, where $\frac{L_s}{2} < L_c$, at a height matching that of the train's roof of 4 m. It is designed to allow trains to temporarily stop or park aside from the main line to facilitate various operations, such as allowing faster trains to pass, changing locomotives or train configurations, or providing a place for trains to wait before entering a congested section of the track [32]. Positioning the BS at the midpoint ensures optimal communication with both trains, while shifting it towards the beginning of the siding loop from any direction would lead to a trade-off, where one direction would receive superior communication, but the other direction would suffer from reduced signal quality or coverage; in this particular case:

- The FSO BS first establishes communication with train operators, coordinating the reservation of the siding loop for one train while the other train waits.
- Once communication is established, then it requests speed adjustments for safe passage and controls train entry and exit.
- Throughout, it continuously monitors train positions, speeds, and activities, implementing safety measures and emergency stop commands as needed to maintain railway system safety and efficiency.

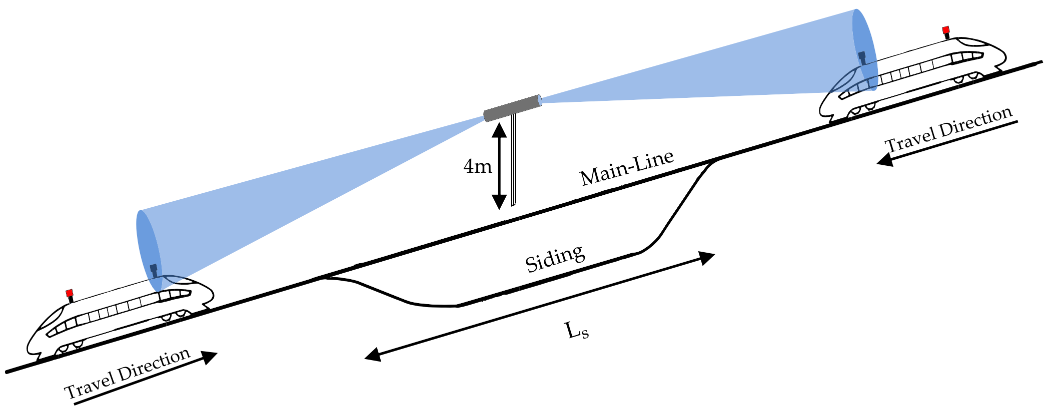

Figure 2. Siding loop model.

4. Channel Model

In our investigations, we consider a G2T FSO communication system that utilizes Intensity Modulation with Direct Detection (IM/DD) using an OOK modulation scheme, which is commonly employed in practical FSO systems. The receiver mounted on the train's roof integrates the photocurrent signal, associated with the incident optical power, by utilizing a detector responsivity R for each bit period. The received electrical signal y is given by [27]:

$$y = hRx + n \tag{3}$$

where x represents the transmitted symbol from BS, h denotes the channel state, and n represents the signal-independent additive white Gaussian noise with variance σ_n^2. The transmitted symbol is $x \in \{0, 2P_t\}$, where P_t represents the average transmitted optical power. The channel state h is assumed to be a composite of three factors multiplicatively independent $h = h_a h_g h_t$ where h_a represents the path loss, h_g represents the attenuation due to geometric spread and pointing errors, and h_t represents the attenuation due to atmospheric turbulence.

4.1. Path Loss

The attenuation of laser power through the atmosphere under the exponential Beer–Lambert law is given by [17]:

$$h_a(z) = \exp(-\sigma z) \tag{4}$$

where σ is the total extinction coefficient. The extinction coefficient is determined by the combined effects of laser photon absorption and scattering caused by different aerosols and gaseous molecules present in the atmosphere. These factors contribute to the overall degradation of the optical signal during transmission.

4.2. Atmospheric Turbulence

The atmospheric turbulence present in Neom city, Tabuk, Saudi Arabia, is considered, as shown in Figure 3. Due to its location, Neom experiences unique climatic conditions that differ from the surrounding desert area. One notable aspect of this city is its geographical diversity, which includes both mountain ranges and sandy beaches. This geographic variation contributes to the presence of atmospheric turbulence in the region, which can impact wireless communication systems. The interaction between the mountainous and coastal environments can lead to changes in atmospheric conditions, such as varying wind patterns and turbulence levels [33,34]. Numerous statistical models have been put forward for characterizing atmospheric fading, aiming to investigate the impact of turbulence-induced fading on the performance of FSO systems. These models are employed to study and analyze the effects caused by atmospheric turbulence on FSO system performance. For weak-to-moderate turbulence conditions, the intensity fluctuation is modeled as a log-normal distribution. For strong turbulence conditions, a Gamma–Gamma distribution is used for the atmospheric fading model (we agree that the adaptation of the LN and GG channels was necessary for a fair comparison with the models in the literature [30], as these models also consider these channels. By employing consistent channel models, we can accurately compare the performance and advantages of different systems). As a result, the Probability Density Function (PDF) is defined as [17]:

$$f_{h_t}(h_t) = \begin{cases} \frac{1}{h_t\sqrt{8\pi\sigma_X^2}} \exp\left(-\frac{(\ln(h_t)-2\mu)^2}{8\sigma_X^2}\right), & \text{for LN} \\ \frac{2(\alpha\beta)^{\frac{\alpha+\beta}{2}}}{\Gamma(\alpha)\Gamma(\beta)h_t} h_t^{\frac{\alpha+\beta}{2}} K_{\alpha-\beta}\left(2\sqrt{\alpha\beta h_t}\right), & \text{for GG} \end{cases}$$

where $\Gamma(a) = \int_0^\infty u^{a-1}e^{-u}du$ and $K_j(.)$ are the Gamma function and the modified Bessel function of the second kind of order j, respectively, $\sigma_X^2 = 1.23\, C_n^2\, k^{\frac{7}{6}}\, z^{\frac{11}{6}}$ is the log irradiance variance, $\mu = -\sigma_X^2$, C_n^2 is the refraction structure's index, and $k = 2\pi/\lambda$ is the optical wave number with wavelength λ. Also, the parameters α and β are the effective number of large-scale and small-scale eddies of scattering environment, respectively [34].

$$\alpha = \left[\exp\left(\frac{0.49\sigma_x^2}{\left(1 + 1.11\sigma_x^{12/5}\right)^{\frac{7}{6}}}\right) - 1\right]^{-1} \tag{7a}$$

$$\beta = \left[\exp\left(\frac{0.51\sigma_x^2}{\left(1+1.11\sigma_x^{12/5}\right)^{\frac{5}{6}}}\right) - 1\right]^{-1} \tag{7b}$$

Figure 3. Location of Neom City [35].

4.3. Pointing Misalignment

In the context of the G2T communication system, which operates in an environment filled with mechanical vibrations, both from train movements and external disturbances, misalignment and pointing errors may occur. A gaussian beam propagates over distance z from the BS to a circular detection aperture with radius a, and the instantaneous radial displacement is between the beam centroid and the detector center r. Approximating the collected power fraction at the receiver as [36]:

$$h_g \approx A_0 \exp\left(-\frac{2r^2}{w_{z_{eq}}^2}\right) \tag{8}$$

where $A_0 = [\mathrm{erf}(v)]^2$ is the fraction of the collected power at $r = 0$, $v = \sqrt{\pi/2}\frac{a}{w_z}$ is the aperture radius to beamwidth ratio, and $w_{z_{eq}}$ is the equivalent beamwidth $w_{z_{eq}}^2 = w_z^2 \frac{\sqrt{\pi}\mathrm{erf}(v)}{2v\ \exp(-v^2)}$. The beamwidth w_z at distance z is given as:

$$w_z \approx w_o\sqrt{1+\left(\frac{\lambda z}{\pi w_o^2}\right)^2} \tag{9}$$

where w_o is the beam waist at $z = 0$.

A Rayleigh distribution is used to model the radial displacement *r* at the receiver [36]:

$$f_r(r) = \frac{r}{\sigma_s^2}\exp\left(-\frac{r^2}{2\sigma_s^2}\right),\ r > 0 \tag{10}$$

where σ_s^2 is the jitter variance at the receiver.

5. Performance Analysis

5.1. SNR

The instantaneous receiver SNR is defined as [36,37]:

$$\gamma_s = \frac{2P_t^2R^2h^2}{\sigma_n^2} \tag{11}$$

and is random due to the fluctuation of h, while the average SNR is:

$$\overline{\gamma}_s = \frac{2P_t^2R^2}{\sigma_n^2}E[h]^2 \tag{12}$$

where E[.] is the statistical expectation.

5.2. LN BER

The BER for NRZ-OOK can be denoted as a function of the SNR as [38]:

$$\text{BER}_{\_\text{OOK}} = \frac{1}{2}\text{erfc}\left(\frac{1}{2\sqrt{2}}\sqrt{\text{SNR}}\right) = Q\left(\frac{1}{2}\sqrt{\text{SNR}}\right) \tag{13}$$

where $\text{erf}(x) = \frac{2}{\sqrt{\pi}}\int_0^x e^{-t^2}dt$ indicates the error function, and $Q(x) = \frac{1}{2\pi}\int_x^\infty \exp(-u^2/2)du$ is the Q function.

The fluctuation in intensity within the FSO channel has a notable effect on the performance of the bit error rate. Considering the presence of channel turbulence and detector noise, the average BER can be described as [39]:

$$\text{BER} = \int_0^\infty \text{BER}_{\_\text{OOK}}\, f_{h_t}(h_t)\, dh_t \tag{14}$$

Then, the average BER for an OOK modulation over a LN channel can be obtained as:

$$\text{BER} = \int_0^\infty Q\left(\frac{1}{2}\sqrt{\text{SNR}}\right)\frac{1}{h_t\sqrt{8\pi\sigma_X^2}}\exp\left(-\frac{(\ln(h_t)-2\mu)^2}{8\sigma_X^2}\right)dh_t \tag{15}$$

Using the Gauss–Hermite quadrature integration approximation $\int_{-\infty}^{\infty} f(x)\exp(-x^2)dx \approx \sum_{i=1}^{N} w_i\, f(x_i)$, where x_i and w_i are the roots and the weights of the Hermite polynomial of order N, we obtain the BER as [40]:

$$P_e \approx \frac{1}{\sqrt{\pi}}\sum_{i=1}^{N} w_i Q\left(\sqrt{\frac{\text{SNR}}{2}}\exp\left(-2\sigma_X^2 + x_i\sqrt{8\sigma_X^2}\right)\right) \tag{16}$$

5.3. GG BER

The average BER for an OOK modulation over a GG channel can be obtained as:

$$\text{BER} = \int_0^\infty Q\left(\frac{1}{2}\sqrt{\text{SNR}}\right)\frac{2(\alpha\beta)^{\frac{\alpha+\beta}{2}}}{\Gamma(\alpha)\Gamma(\beta)h_t}h_t^{\frac{\alpha+\beta}{2}}K_{\alpha-\beta}\left(2\sqrt{\alpha\beta h_t}\right)dh_t \tag{17}$$

Using the relation between Bessel function and Meijer's G-function in [32], the *BER* can be expressed as [41]:

$$P_e \approx \frac{2^{\alpha+\beta-3}}{\pi^{\frac{3}{2}}\Gamma(\alpha)\Gamma(\beta)}G_{5,2}^{2,4}\left[\left(\frac{2}{\alpha\beta}\right)^2 \times \text{SNR}\left|\begin{matrix}\frac{2-\alpha}{2}, \frac{1-\alpha}{2}, \frac{2-\beta}{2}, \frac{1-\beta}{2}, 1\\ 0, \frac{1}{2}\end{matrix}\right.\right] \tag{18}$$

where $G_{p,q}^{m,n}\left(\begin{matrix}a_1, \ldots, a_p\\ b_1, \ldots, b_q\end{matrix}\middle| z\right)$ presents the Meijer's G-function.

6. Numerical Results and Discussion

Numerical evaluations were performed on the proposed model using MATLAB®. Table 1 contains the parameters associated with the system model. The selection of these parameters was based on three key considerations. Firstly, we analyzed the laser beam, as in [19]. Secondly, we considered the channel model, as in [36]. Lastly, we incorporated the atmospheric turbulence parameters specific to Neom city according to the methodology outlined in [34]. Additionally, the system operates at an 850 nm wavelength, which ensures safety and is suitable for deployment in public areas. This wavelength falls within the near-infrared region known for its lower risk of adverse effects on human eyes. Moreover, we considered employing lasers classified as Class 1 or Class 1M, which are deemed safe for direct human exposure according to international laser safety standards. Class 1 lasers are considered safe under normal operating conditions and pose no hazards. They are considered incapable of producing damaging levels of laser radiation. Class 1M lasers, on the other hand, are safe for direct viewing as long as they are not observed through magnifying optics [42]. We assumed that the handover delay, indicating the time needed for each transceiver on the train to establish a connection with the BS, is 130 ms, as indicated in [21,24]. Our proposed model was subjected to a comprehensive evaluation of system performance, considering both LN and GG channels from received SNR and BER perspectives. Additionally, a comparative analysis was performed, in which our results were compared with those of other existing FSO systems.

Table 1. System parameters.

Parameter	Symbol	Value
Extinction Coefficient	σ	0.44 dB/km
Wavelength	λ	850 nm
Optical Transmission Power	P_t	40 mW
Additive Noise Standard Deviation	σ_n	10^{-7} A/Hz
PD Responsivity	R	0.5 A/W
Detector Radius	a	10 cm
Jitter Standard Deviation	σ_s	30 cm
Vertical Distance	L_v	3 m
Horizontal Distance	L_H	95 m
Train Length	L_T	200 m
TX/RX Tilting Angle	γ	2.5 degree
HST Speed	V	300 km/h
Refraction Structure's Index (Weak-to-Strong Turbulence)	C_n^2	1.26×10^{-14} $m^{-2/3}$, 5.9×10^{-14} $m^{-2/3}$

We evaluated the BER performance of our proposed model using the commonly employed OOK modulation technique. Furthermore, in order to conduct a fair comparison with the models presented in [30], which involve an intermediate node between the transmitter and receiver, we evaluated the BER performance using the 4-PAM modulation technique for these models to maintain similar throughput. In the case of OOK, each time slot represents one bit since our model is a direct FSO system. On the other hand, we employed 4-PAM modulation technique for RIS- and relay-assisted FSO systems, which involves an intermediate node, where two bits are transmitted over two time slots. Therefore, both modulation techniques maintain a similar throughput of one bit per one time slot [43].

Figure 4a,b illustrate the received SNR versus the coverage distance along the track for a single transceiver FSO, RIS, and relay-assisted FSO communication systems in the presence of LN and GG channels, respectively. As shown, the single transceiver model demonstrates a superior coverage distance for both LN and GG channels, as it achieves a high received SNR at each BS compared to RIS- and relay-assisted FSO.

One crucial reason for this improvement is that the intermediate RIS or relay node is positioned in close proximity to the transmitter, to provide an early signal boost in the transmission path, compensating for initial signal losses and atmospheric effects that may occur over longer distances. Additionally, aligning the node with the transmitter is relatively easier compared to aligning it with the receiver, simplifying the alignment process and reducing misalignment errors [30]. By expanding the coverage distance provided by each dual transceiver BS, the number of required BSs and handover frequency can be minimized for Neom's HSR line. Additionally, these findings emphasize the importance of channel consideration, as the chosen channel significantly impacts the system's performance over longer distances, particularly in turbulent conditions. Therefore, a careful consideration of both LN and GG channels is essential for designing FSO systems in G2T applications, ensuring reliable communication across various turbulence scenarios.

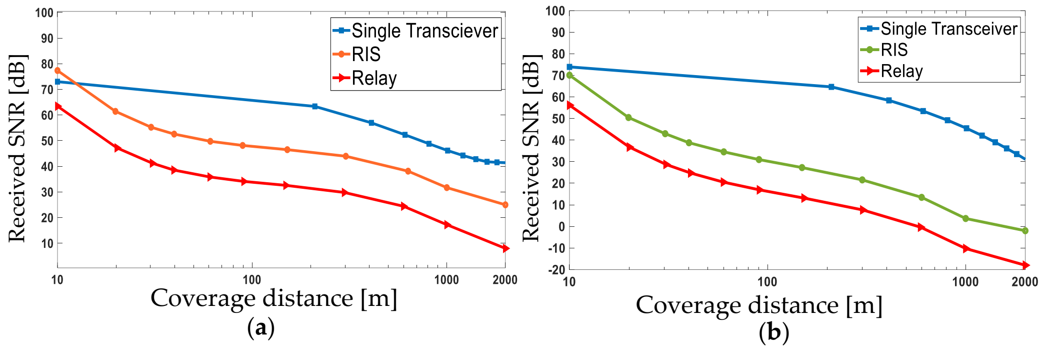

Figure 4. Received SNR vs. coverage distance through: (**a**) LN channel; (**b**) GG channel.

The BER performance of the dual transceiver model for NRZ-OOK with LN and GG distributed channel models for different propagation distances are presented in Figure 5a,b, respectively. The BER values are determined using Equations (16) and (18) for weak-to-moderate and strong turbulence, respectively. The results indicate that achieving a satisfactory BER under large propagation distances and strong turbulence requires high power. It is clearly depicted that the BER for the considered channels shows an improvement with increased SNR. Whether the turbulence strength is weak-to-moderate or strong, the consistency between the results obtained from numerical simulations and theoretical analysis is good. Monte Carlo computer simulations with 10^{10} iterations were used to obtain the simulated BER.

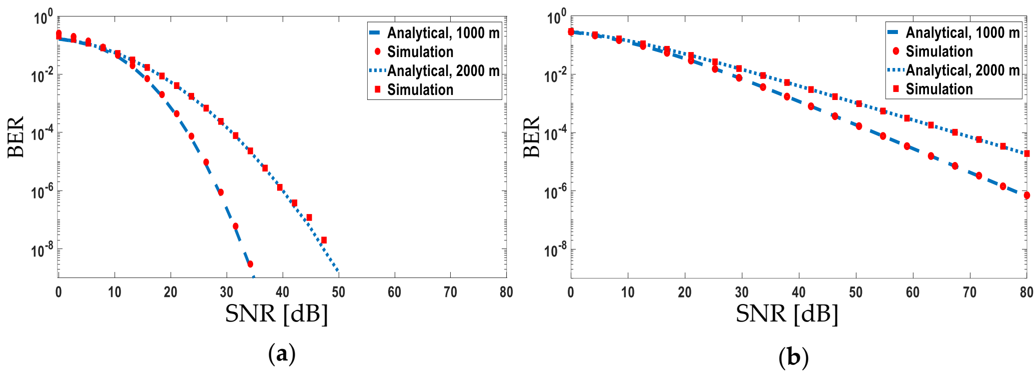

Figure 5. BER vs. received SNR of dual transceiver through: (**a**) LN channel; (**b**) GG channel for different propagation distances.

In Figure 6a,b, we present a comparison of the BER dual transceiver FSO, RIS-assisted FSO, and relay-assisted FSO under weak-to-moderate and strong atmospheric turbulence conditions, respectively [40,44,45]. It is evident that the dual transceiver model outperforms the relay-assisted FSO in both LN and GG channels. Furthermore, the RIS-assisted FSO exhibits a distinct performance variation between lower and higher SNR regimes. In high SNR conditions, the received signal strength is relatively strong compared to the noise level. This advantageous scenario allows the RIS to manipulate the signal more effectively. By optimizing the signal environment through adjusting the phase and amplitude of the reflected signals, the RIS enhances the signal power and quality [46]. Consequently, the RIS contributes to improving the received signal power, reducing fading effects, and enhancing the overall system performance. Additionally, it is worth noting that in high SNR regimes, the impact of channel impairments, such as atmospheric turbulence-induced fading and multipath propagation, is relatively reduced. This reduction can be attributed to the stronger received signal strength, which helps mitigate the adverse effects of these impairments. As a result, the RIS system's performance is enhanced in high SNR regimes.

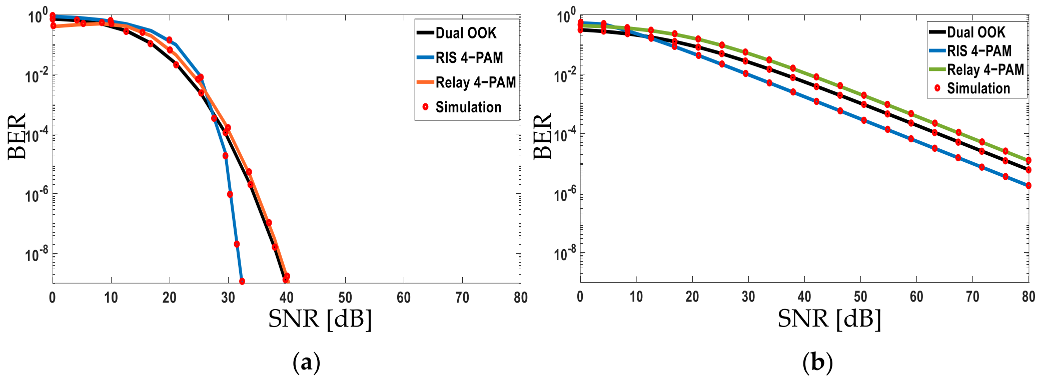

Figure 6. BER vs. received SNR of different models through: (**a**) LN channel; (**b**) GG channel.

Table 2 provides a comprehensive overview of the required BSs for dual transceiver, RIS, and relay FSO communication systems, regarding Figures 4 and 6. Considering the HSR track of Neom city spans 170 km, we initiate the analysis by extracting the received SNR values from Figure 6 based on the specified BER detailed in the table for both channels. Subsequently, consulting Figure 4 allows us to ascertain the coverage distance values corresponding to the received SNR values. By dividing the total length of the 170 km line track by the determined coverage distances, we can accurately calculate the number of required BSs for each model. This approach ensures a systematic assessment of the deployment requirements, offering valuable insights into the optimal configuration of the G2T communication systems. As an example, let us consider LN RIS model as outlined in Table 2:

Table 2. Base station characteristics.

Channel Model	**LN**			**GG**		
BER	10^{-9}			10^{-3}		
System Model	Dual Transceiver	RIS	Relay	Dual Transceiver	RIS	Relay
Received SNR [dB]	40	33	41	50	47	55
Coverage Distance [m]	4190	1000	31	1790	25	10
Required BSs	41	170	5484	95	6800	17,000

At a BER of 10^{-9}, Figure 6a indicates a received SNR of 33 db. Consulting Figure 4a reveals that the coverage distance at 33 dB is 1000 m. With our consideration of a 170 km line track, the number of required BSs results in 170 BSs.

The results clearly demonstrate the advantages of the dual transceiver FSO system in terms of coverage distance and infrastructure efficiency in railway settings, leading to a significant reduction of up to 76% and 99% in the number of required BSs in the LN channel besides 98% and 99% in the GG channel compared to RIS-assisted FSO and relay-assisted FSO systems, respectively. The expansion of the coverage area not only minimizes handover processes but also has the potential to decrease CAPEX costs and required infrastructure, as fewer BSs are required to be deployed along the rail line in the city.

7. Conclusions

In this work, we introduced a dual transceiver FSO communication system for Neom's HST, incorporating both LN and GG channel models to accurately represent turbulence effects in the city. The research made significant contributions to the practical field by expanding the scope to include the siding loop in the single-line track. Through the numerical results, we demonstrated that the dual transceiver model achieved a larger coverage distance compared to RIS- and relay-assisted FSO systems. Furthermore, the evaluation of the BER performance confirmed the improvement with increased SNR for both the LN and GG channel models. The validity of the main results was confirmed through Monte Carlo simulations. In conclusion, our research presents a novel and efficient solution for Neom's HST that surpasses existing systems in terms of received SNR, coverage area, and required infrastructure. The incorporation of both LN and GG channel models, as well as the consideration of real-world scenarios, contributes to the practicality and effectiveness of the proposed system in the HSR environment of the Neom smart city. Further research will include underground (tunnel) scenarios, where BSs are located in the ceiling of the tunnel. This expansion of research will enable a comprehensive understanding of the system's capabilities and effectiveness in various challenging environments, ultimately providing valuable insights for the implementation of FSO technology in Neom's smart city infrastructure.

Author Contributions: Conceptualization, Y.E. and A.S.A. methodology, A.M.; software, M.A.; validation, E.-H.M.A., Y.E., and A.S.A.; formal analysis, A.M.; investigation, M.A.; resources, A.S.A.; data curation, Y.E.; writing—original draft preparation, Y.E.; writing—review and editing, A.M.; visualization, A.S.A.; supervision, M.A.; project administration, E.-H.M.A.; funding acquisition, A.S.A. All authors have read and agreed to the published version of the manuscript.

Funding: This work is supported by the Research, Development and Innovation Authority (RDIA), Saudi Arabia, grant number 13010-Tabuk-2023-UT-R-3-1-SE, and by the Deanship of Scientific Research, University of Tabuk, Saudi Arabia, grant number RGP-S-1441-0148.

Institutional Review Board Statement: Not applicable.

Informed Consent Statement: Not applicable.

Data Availability Statement: No data were generated in the presented research.

Acknowledgments: The authors extend their appreciation to the Saudi National Center for Meteorology for providing weather data for the study.

Conflicts of Interest: The authors declare no conflicts of interest.

References

1. Sharifi, A.; Allam, Z.; Elias, S.; Reza, A. Smart cities and sustainable development goals (SDGs): A systematic literature review of co-benefits and trade-offs. *Cities* **2024**, *146*, 104659. [CrossRef]
2. Mavlutova, I.; Atstaja, D.; Grasis, J.; Kuzmina, J.; Uvarova, I.; Roga, D. Urban Transportation Concept and Sustainable Urban Mobility in *Smart Cities*: A Review. *Energies* **2023**, *16*, 3585. [CrossRef]
3. Anwar, A.H.M.M.; Oakil, A.T. Smart Transportation Systems in Smart Cities: Practices, Challenges, and Opportunities for Saudi Cities. In *Smart Cities. Studies in Energy, Resource and Environmental Economics*; Springer: Cham, Switzerland, 2023; pp. 315–337.
4. Du, Q.; Yu, H.; Yan, C.; Yang, T. Does High-Speed Rail Network Access Enhance Cities' Innovation Performance? *Sustainability* **2020**, *12*, 8239. [CrossRef]
5. Neom. Available online: https://www.neom.com/en-us/regions/theline (accessed on 30 March 2024).
6. Wu, J.; Fan, P. A Survey on High Mobility Wireless Communications: Challenges, Opportunities and Solutions. *IEEE Access* **2016**, *4*, 450–476. [CrossRef]
7. Ai, B.; Cheng, X.; Kürner, T.; Zhong, Z.D.; Guan, K.; He, R.S.; Xiong, L.; Matolak, D.W.; Michelson, D.G.; Briso-Rodriguez, C. Challenges Toward Wireless Communications for High-Speed Railway. *IEEE Trans. Intell. Transp. Syst.* **2014**, *15*, 2143–2158. [CrossRef]
8. Yaacoub, E.; Alsharoa, A.; Ghazzai, H.; Alouini, M.-S. Seven Challenges for Communication in Modern Railway Systems. *Front. Commun. Netw.* **2021**, *1*, 619527. [CrossRef]
9. Ashraf, M.W.; Idrus, S.M.; Iqbal, F.; Butt, R.A.; Faheem, M. Disaster-Resilient Optical Network Survivability: A Comprehensive Survey. *Photonics* **2018**, *5*, 35. [CrossRef]
10. Mohammadani, K.H.; Butt, R.A.; Memon, K.A.; Pirzado, A.A.; Faheem, M.; Abro, A.; Ali, B.; Ain, N.U. A QoS provisioning architecture of fiber wireless network based on XGPON and IEEE 802.11ac. *J. Opt. Commun.* **2023**, *44*, s1017–s1022. [CrossRef]

11. Butt, R.A.; Waqar Ashraf, M.; Faheem, M.; Idrus, S.M. A Survey of Dynamic Bandwidth Assignment Schemes for TDM-Based Passive Optical Network. *J. Opt. Commun.* **2020**, *41*, 279–293. [CrossRef]
12. Kaushal, H.; Kaddoum, G. Optical Communication in Space: Challenges and Mitigation Techniques. *IEEE Commun. Surv. Tutor.* **2017**, *19*, 57–96. [CrossRef]
13. Safari, M.; Uysal, M. Relay-assisted free-space optical communication. *IEEE Trans. Wirel. Commun.* **2008**, *7*, 5441–5449. [CrossRef]
14. Wang, Y.; Xu, H.; Li, D.; Wang, R.; Jin, C.; Yin, X.Y.; Gao, S.; Mu, Q.; Zuan, L.; Cao, Z. Performance analysis of an adaptive optics system for free-space optics communication through atmospheric turbulence. *Sci. Rep.* **2018**, *8*, 1124. [CrossRef] [PubMed]
15. Youssef, A.A.; Abaza, M.; Alatawi, A.S. LDPC Decoding Techniques for Free-Space Optical Communications. *IEEE Access* **2021**, *9*, 133510–133519. [CrossRef]
16. Wang, K.; Nirmalathas, A.; Lim, C.; Skafidas, E. High-Speed Optical Wireless Communication System for Indoor Applications. *IEEE Photonics Technol. Lett.* **2011**, *23*, 519–521. [CrossRef]
17. Khalighi, M.A.; Uysal, M. Survey on FSO Communication: A Communication Theory Perspective. *IEEE Commun. Surv. Tutor.* **2014**, *16*, 2231–2258. [CrossRef]
18. Urabe, H.; Haruyama, S.; Shogenji, T.; Ishikawa, S.; Hiruta, M.; Teraoka, F.; Arita, T.; Matsubara, H.; Nakagawa, S. High data rate G2T FSO communication system. *Opt. Eng.* **2012**, *51*, 031204. [CrossRef]
19. Paudel, R.; Ghassemlooy, Z.; Le-Minh, H.; Rajbhandari, S. Modelling of free space optical link for ground-to-train communications using a Gaussian source. *IET Optoelectron.* **2013**, *7*, 1–8. [CrossRef]
20. Paudel, R.; Ghassemlooy, Z.; Le Minh, H.; Rajbhandari, S.; Leitgeb, E. Lambertian source modelling of FSO G2T communications. In Proceedings of the 8th International Symposium on Communication Systems, Networks & Digital Signal Processing (CSNDSP), Poznan, Poland, 18–20 July 2012; pp. 1–5.
21. Fan, Q.; Taheri, M.; Ansari, N.; Feng, J.; Rojas-Cessa, R.; Zhou, M.; Zhang, T. Reducing the Impact of Handovers in G2T FSO Communications. *IEEE Trans. Veh. Technol.* **2018**, *67*, 1292–1301. [CrossRef]
22. Han, T.; Ansari, N. RADIATE: Radio over fiber as an antenna extender for high-speed train communications. *IEEE Wirel. Commun.* **2015**, *22*, 130–137. [CrossRef]
23. Kaymak, Y.; Rojas-Cessa, R.; Feng, J.; Ansari, N.; Zhou, M. On Divergence-Angle Efficiency of a Laser Beam in FSO Communications for High-Speed Trains. *IEEE Trans. Veh. Technol.* **2017**, *66*, 7677–7687. [CrossRef]
24. Fan, Q.; Ansari, N.; Feng, J.; Rojas-Cessa, R.; Zhou, M.; Zhang, T. Reducing the Number of FSO Base Stations With Dual Transceivers for Next-Generation G2T Communications. *IEEE Trans. Veh.* **2018**, *67*, 11143–11153. [CrossRef]
25. Mabrouk, W.A.; Abdullah, M.F.L. FSO G2T communications in tropical climate: An overview. *AIP Conf. Proc.* **2017**, *1883*, 020009.
26. Mabrouk, W.A.; Abdullah, M.F.L.; Gismalla, M.S.M. Enhancement of Link Range for FSO Ground to Train Communications Using Multiple Transmitters Concept, 2019. In Proceedings of the International Conference on Information Science and Communication Technology (ICISCT), Karachi, Pakistan, 9–10 March 2019; pp. 1–7.
27. Mohan, N.; Abadi, M.M.; Ghassemlooy, Z.; Zvanovec, S.; Hudson, R.; Bhatnagar, M.R. Sectorised base stations for FSO G2Tcommunications. *IET Optoelectron.* **2020**, *14*, 312–318. [CrossRef]
28. Dabiri, M.T.; Sadough, S.M.S.; Khalighi, M.A. FSO Communication for High Speed Trains: Blind Data Detection and Channel Estimation. In Proceedings of the 11th International Symposium on Communication Systems, Networks & Digital Signal Processing (CSNDSP), Budapest, Hungary, 18–20 July 2018; pp. 1–4.
29. Mohan, N.; Ghassemlooy, Z.; Zvanovec, S.; Abadi, M.M.; Hudson, R.; Bhatnagar, M.R. Relayed FSO Links for G2TCommunications. In Proceedings of the 12th International Symposium on Communication Systems, Networks and Digital Signal Processing (CSNDSP), Porto, Portugal, 20–22 July 2020; pp. 1–6.
30. Agheli, P.; Beyranvand, H.; Emadi, M.J. High-Speed Trains Access Connectivity Through RIS-Assisted FSO Communications. *J. Light. Technol.* **2022**, *40*, 7084–7094. [CrossRef]
31. Feng, C. An Improved of Information Transmission Mode of High-Speed Railway Centralized Traffic Control System. In Proceedings of the 11th International Conference on Measuring Technology and Mechatronics Automation (ICMTMA), Qiqihar, China, 28–29 April 2019; pp. 327–331.
32. Pachl, J. *Railway Signalling Principles*, 2nd ed.; TU Braunschweig: Braunschweig, Germany, 2021.
33. Farag, A.A. The Story of NEOM City: Opportunities and Challenges. In *New Cities and Community Extensions in Egypt and the Middle East*; Springer: Berlin/Heidelberg, Germany, 2019; pp. 35–49.
34. Alatawi, A.S.; Youssef, A.A.; Abaza, M.; Uddin, M.A.; Mansour, A. Effects of Atmospheric Turbulence on Optical Wireless Communication in NEOM Smart City. *Photonics* **2022**, *9*, 262. [CrossRef]
35. Saud, M.M.A. *Sustainable Land Management for NEOM Region*; Springer: Berlin/Heidelberg, Germany, 2020.
36. Farid, A.A.; Hranilovic, S. Outage Capacity Optimization for FSO Links With Pointing Errors. *J. Light. Technol.* **2007**, *25*, 1702–1710. [CrossRef]
37. Gappmair, W.; Nistazakis, H.E. Subcarrier PSK Performance in Terrestrial FSO Links Impaired by Gamma-Gamma Fading, Pointing Errors, and Phase Noise. *J. Light. Technol.* **2017**, *35*, 1624–1632. [CrossRef]
38. Malik, S.; Sahu, P.K. Performance Analysis of FSO Communication System Using Different Modulation Schemes over Weak to Strong Atmospheric Turbulence Channels. In *Optical and Wireless Technologies*; Springer: Singapore, 2020; Volume 546.
39. Zhang, Y.; Yang, Y.; Hu, B.; Yu, L.; Hu, Z.-D. Average BER and outage probability of the G2T OWC link in turbulence with rain. *Opt. Commun.* **2017**, *398*, 85–90, ISSN 0030-4018. [CrossRef]

40. Abaza, M.; Mesleh, R.; Mansour, A.; Aggoune, H.M. Performance Analysis of MISO Multi-Hop FSO Links over Log-Normal Channels with Fog and Beam Divergence Attenuations. *Opt. Commun.* **2015**, *334*, 247–252. [CrossRef]
41. Xu, Z.; Xu, G.; Zheng, Z. BER and Channel Capacity Performance of An FSO Communication System over Atmospheric Turbulence with Different Types of Noise. *Sensors* **2021**, *21*, 3454. [CrossRef] [PubMed]
42. Haley, D.; Pratt, O. Basic Principles of Lasers. *Anaesth. Intensive Care Med.* **2017**, *18*, 648–650. [CrossRef]
43. Fath, T.; Haas, H. Performance Comparison of MIMO Techniques for Optical Wireless Communications in Indoor Environments. *IEEE Trans. Commun.* **2013**, *61*, 733–742. [CrossRef]
44. Duong, H.A.; Vuong, C.D.; Dang, D.T. Average symbol error rate analysis of reconfigurable intelligent surfaces-assisted free-space optical link over log-normal turbulence channels. *Int. J. Electr. Comput. Eng.* **2023**, *13*, 571–578.
45. Ai, D.H.; Dang, D.T.; Dang, Q.H.; Le Kim, T. Analysis on the performance of pointing error effects for RIS-aided FSO link over gamma-gamma channels. *TELKOMNIKATelecommun. Comput. Electron. Control.* **2023**, *21*, 718–724. [CrossRef]
46. ElMossallamy, M.A.; Zhang, H.; Song, L.; Seddik, K.G.; Han, Z.; Li, G.Y. Reconfigurable Intelligent Surfaces for Wireless Communications: Principles, Challenges, and Opportunities. *IEEE Trans. Cogn. Commun. Netw.* **2020**, *6*, 990–1002. [CrossRef]